
A COMPARATIVE STUDY OF LOSS FUNCTIONS: TRAFFIC PREDICTIONS IN REGULAR AND CONGESTION SCENARIOS

A PREPRINT

Yangxinyu Xie

Department of Statistics and Data Science
University of Pennsylvania
Philadelphia, PA
xinyux@wharton.upenn.edu

Tanwi Mallick

Mathematics and Computer Science Division
Argonne National Laboratory
Lemont, IL
tmallick@anl.gov

August 30, 2023

ABSTRACT

Spatiotemporal graph neural networks have achieved state-of-the-art performance in traffic forecasting. However, they often struggle to forecast congestion accurately due to the limitations of traditional loss functions. While accurate forecasting of regular traffic conditions is crucial, a reliable AI system must also accurately forecast congestion scenarios to maintain safe and efficient transportation. In this paper, we explore various loss functions inspired by heavy tail analysis and imbalanced classification problems to address this issue. We evaluate the efficacy of these loss functions in forecasting traffic speed, with an emphasis on congestion scenarios. Through extensive experiments on real-world traffic datasets, we discovered that when optimizing for Mean Absolute Error (MAE), the MAE-Focal Loss function stands out as the most effective. When optimizing Mean Squared Error (MSE), Gumbel Loss proves to be the superior choice. These choices effectively forecast traffic congestion events without compromising the accuracy of regular traffic speed forecasts. This research enhances deep learning models' capabilities in forecasting sudden speed changes due to congestion and underscores the need for more research in this direction. By elevating the accuracy of congestion forecasting, we advocate for AI systems that are reliable, secure, and resilient in practical traffic management scenarios.

Keywords Deep Learning, Spatiotemporal Graph Neural Networks, Traffic Prediction, Loss Function

1 Introduction

With the advent of machine learning, spatiotemporal Graph Neural Networks (GNN) have emerged as a promising tool, delivering state-of-the-art results in short-term traffic speed forecasting Li et al. [2018], Wu et al. [2019], Shao et al. [2022], Lablack and Shen [2023]. However, a significant challenge remains: current deep learning models trained using loss functions such as Mean Absolute Error (MAE) or Mean Squared Error (MSE) struggle to forecast rarer instances Ding et al. [2019], Ribeiro and Moniz [2020]. While these advanced GNNs excel at predicting regular traffic speeds, they often fall short in forecasting traffic congestion.

Fig. 1 highlights a regularly congested location in Los Angeles. Although speeds generally fluctuate between 60 and 70 mph, the traffic speed histogram reveals a pronounced bimodal distribution. This bimodality violates the normality assumptions baked into loss functions such as MAE and MSE. Moreover, as shown in Fig. 2, the levels of bimodality significantly differ throughout the road network, making accurate traffic speed forecasting even more complex.

Traffic congestion not only results in significant economic losses due to increased travel times and operational inefficiencies but also poses challenges in ensuring safe and efficient transportation systems. A robust and responsible AI system should accurately forecast normal, elevated, and extreme levels of congestion as it is crucial for enhancing traffic control, optimizing routing, and identifying innovative solutions to evolving patterns of congestion Bishop [2005], Tang and Gao [2005], Teklu et al. [2007].

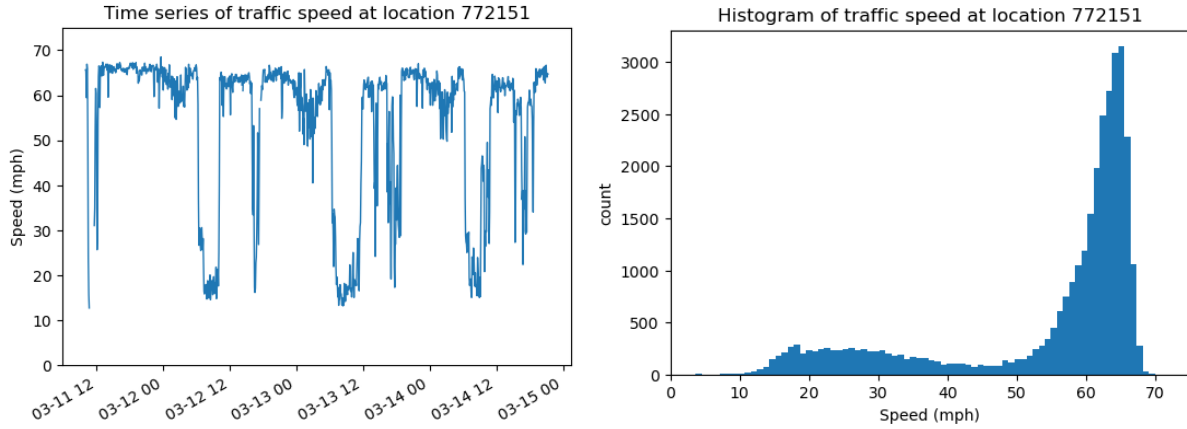


Figure 1: Historical traffic speed at sensor location 772151. Left: time series from March 11th 2012 to March 14th 2012. Right: histogram with observations from March 1st 2012 to June 30th 2012.

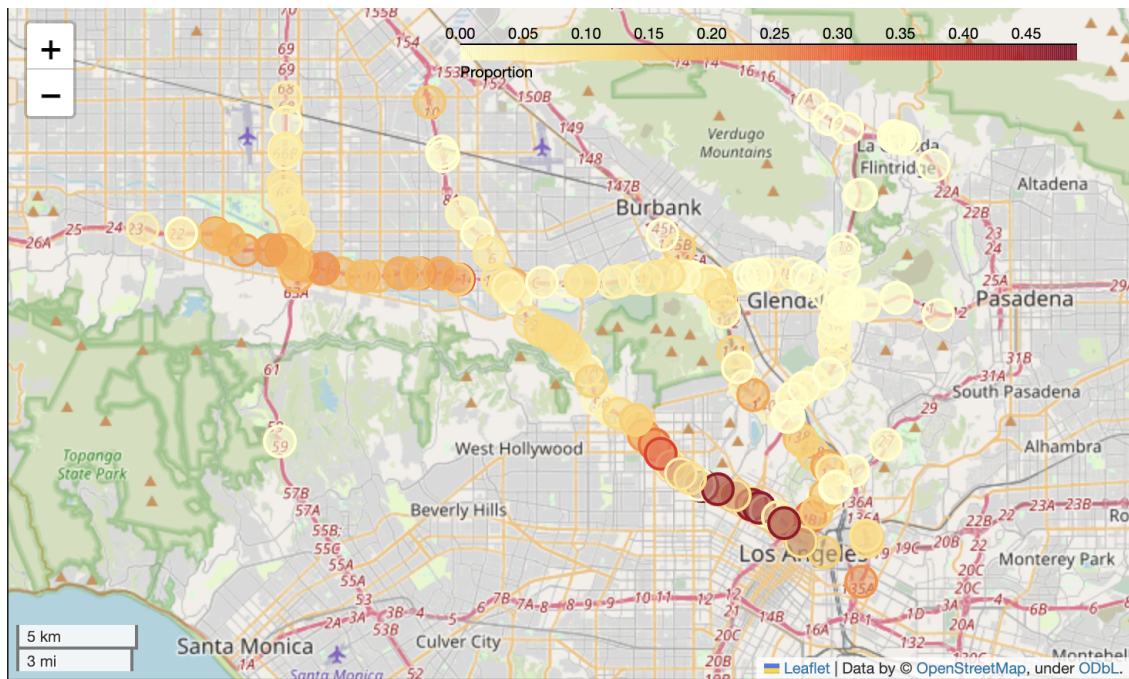


Figure 2: The visualization of the levels of bimodality across different locations in the METR-LA dataset. The darker the color, the more severe the bimodality. The exact definition of the “proportion” in the legend is presented in the Methods section.

In the literature of time series forecasting, researchers have proposed innovative loss functions based on extreme value theory to better account for rare events Ding et al. [2019], Zhang et al. [2021], Kozerawski et al. [2022]. However, traffic congestion does not align perfectly with this theory: unlike extreme weather or pollution, traffic congestions occur more regularly throughout the year, as seen in Fig. 1, and possess structured seasonal and spatial dependencies that often violate the assumptions of the extreme value theory. Other loss functions, inspired by imbalanced classification problems in computer vision, have been proposed Ribeiro and Moniz [2020], Yang et al. [2021], Ren et al. [2022]. These loss functions aim to restore a balanced prediction from imbalanced training samples. However, imbalanced regression is still in an early stage and lacks an effective approach. Furthermore, these loss functions have only been tested in vision-related tasks.

Nevertheless, these loss functions may enhance current deep learning models’ abilities to predict abrupt traffic speed changes due to congestion. Unfortunately, no studies have conducted a systematic comparison of these loss functions. Moreover, most of these loss functions have not been previously employed in traffic forecasting scenarios.

In this paper, we contribute to the practice of safe, robust, and responsible AI-based systems by addressing this gap. We incorporate eight loss functions from multiple studies into two state-of-the-art spatiotemporal graph neural networks. We evaluate their efficacy in forecasting traffic speed for highway networks using three distinct metrics. These metrics will not only assess the overall performance of these loss functions but also their efficacy in pinpointing traffic congestion, ensuring a more reliable and robust AI system for real-world traffic management applications.¹

2 Related Work

Spatiotemporal GNNs in Traffic Forecasting. Urban traffic inherently exhibits a non-Euclidean topological structure. To decode this structure, spatiotemporal GNNs capture spatial dependencies via a diffusion process on graphs Li et al. [2018], Wu et al. [2019] and temporal patterns using sequence-to-sequence recurrent neural networks Cho et al. [2014], Yu and Koltun [2016]. Subsequent research has refined these models on benchmark datasets like METR-LA and PEMS-BAY Zhang et al. [2018], Yu et al. [2018], Shao et al. [2022], Lablack and Shen [2023]. Other studies have scaled these models to accommodate larger road networks Mallick et al. [2020a,b], Zheng et al. [2023], and integrated advanced techniques like transfer learning Mallick et al. [2021], Huang et al. [2021] and uncertainty quantification Mallick et al. [2022]. Nonetheless, spatiotemporal GNNs struggle to accurately forecast congestion, primarily because the distribution of traffic speed significantly deviates from normality, which compromises the effectiveness of standard loss functions like MAE and MSE.

Heavy Tail Analysis and Extreme Value Theory. Heavy-tailed random variables, characterized by a high likelihood of significant deviations from the mean, are often observed in road traffic patterns, as exemplified in Fig. 1. Statistical techniques in heavy tail analysis often overlap with extreme value theory and have been successful in modelling rare impactful events like floods or heatwaves Haan and Ferreira [2006], Tanarhte et al. [2015]. In the context of loss functions, Ding et al. [2019] introduced Extreme Value Loss (EVL) to predict the future occurrence of extreme events. However, this loss function is based on a binary classification layer, making it difficult to implement for regression problems. To circumvent this, Zhang et al. [2021] proposed a generalized EVL framework inspired by the kernel density estimator (KDE) and introduced the Gumbel Loss and the Fréchet Loss functions. Nonetheless, Fréchet Loss is only well-defined only for one-sided extreme events, making it unsuitable for traffic time series data. Meanwhile, Kozerawski et al. [2022] proposed two moment-based tailedness measurement concepts: Pareto loss and Kurtosis Loss. However, the authors did not specify how to choose the hyperparameters for the generalized Pareto distribution within the Pareto loss; thus, we omit the Pareto loss from our study. Quantile regression, a method estimating the conditional quantiles of a response variable Koenker [2005], has also been recently adapted into deep learning to model extreme events Wambura et al. [2020]. These novel loss functions have demonstrated superior efficacy in identifying infrequent events in a time series. It is thus interesting to investigate their potential in improving traffic forecasting. Nonetheless, as remarked in the Introduction, the random variable governing the observed traffic speed, albeit heavy-tailed, does not exactly conform to classical extreme value theory.

Imbalanced Regression. Complimentary to heavy tail analysis, imbalanced regression focuses on restoring a balanced prediction from imbalanced training samples. Although a crucial area, it remains under-explored. Recent approaches focus on estimating the prior density distribution of training sets and then reweighting Yang et al. [2021], Steininger et al. [2021]. Yet, it remains uncertain how to effectively estimate the prior density of traffic speed data, given their intricate structure of interdependencies. In the field of computer vision, several loss functions, inspired by Focal Loss, have been proposed and these methods do not require any prior knowledge about the distribution of training labels. Shrinkage Loss utilizes a sigmoid-based function to recalibrate loss terms Lu et al. [2018]. This approach was later generalized by Yang et al. [2021]. Most recently, Ren et al. [2022] proposed the Balance MSE (bMSE) Loss, which bears a resemblance to the logit adjustment techniques employed in the literature on imbalanced classification. Despite their success in vision-related tasks, the efficacy of these innovative loss functions in traffic forecasting remains an open question, a gap which our study seeks to address.

3 Methods

The goal of traffic forecasting is to predict the future traffic speed given previously observed traffic speed from D correlated sensor locations on the road network. Concretely, at each time step, given the representation of a graph G capturing the spatial correlation among the sensor locations and the traffic speed data at D locations for the previous S

¹The source code is available at <https://github.com/Xieyangxinyu/A-Comparative-Study-of-Loss-Functions-Traffic-Predictions-in-Regular-and-Congestion-Scenarios>

time steps, the problem is to learn a function f that outputs a 2-dimensional matrix, which represents the traffic speed data at D locations for the next T time steps. For each $d = 1, \dots, D$ and $t = 1, \dots, T$, we let y_{dt} denote the observed value at location d and time t and \hat{y}_{dt} denote the predicted value by the model. In this section, we first define each loss function included in this study. Then, we introduce the metrics that will collectively examine the models' overall performance as well as effectiveness at identifying congestion.

3.1 Loss Functions

For our study, we categorize the loss functions into three distinct groups: first-order losses, second-order losses, and Kurtosis Loss. First-order losses, which impose an L-1 penalty on large errors, include MAE, MAE-Focal, Quantile, and Huber Loss. In general, the L-1 penalty is resistant to values that deviate from the mean. Second-order losses, applying an L-2 penalty on large errors, consist of MSE, MSE-Focal, Balanced MSE, and Gumbel Loss. Unlike the L-1 penalty, the L-2 penalty adjusts the model to account for "outliers," sometimes at the expense of accuracy on other samples. Except for the balanced MSE Loss, we give the definition of each loss function at the level of each sample.

Mean absolute error (MAE) and Mean squared error (MSE): The MAE is defined as: $\frac{1}{D} \frac{1}{T} \sum_{d=1}^D \sum_{t=1}^T |y_{dt} - \hat{y}_{dt}|$. The MSE is defined as: $\frac{1}{D} \frac{1}{T} \sum_{d=1}^D \sum_{t=1}^T (y_{dt} - \hat{y}_{dt})^2$. In the literature, MAE loss is typically preferred when forecasting traffic with spatiotemporal GNNs because it often induces better overall performance. However, MSE is more sensitive to outliers since it squares the error and exaggerates the effect of outliers.

Focal Loss: Focal Loss applies a modulating term to the cross entropy loss in order to focus learning on harder, rarer examples Lin et al. [2017], Lu et al. [2018]. We adopt a more general variation of the Focal Loss for regression proposed by Yang et al. [2021]. It is defined as $\frac{1}{D} \frac{1}{T} \sum_{d=1}^D \sum_{t=1}^T \sigma(|\beta \cdot e_{lt}|)^\gamma e_{lt}$, where $\sigma(\cdot)$ is the sigmoid function, β, γ are the hyperparameters and e_{lt} is the error at location l and at time t . We choose two errors for e_{lt} : absolute error: $e_{lt} = |y_{dt} - \hat{y}_{dt}|$, and squared error: $e_{lt} = (y_{dt} - \hat{y}_{dt})^2$. We refer to the Focal Loss function with the absolute error as **MAE-Focal** and the one with the squared error as **MSE-Focal**.

Huber Loss: Huber Loss is a loss function used in robust regression. It combines MAE with MSE so that it is less sensitive to outliers in data than the MSE Huber [1992]. Huber Loss is defined as $\sum_{d=1}^D \sum_{t=1}^T L_{\beta,d,t}$ where

$$L_{\beta,d,t} = \begin{cases} (y_{dt} - \hat{y}_{dt})^2/2 & \text{if } |y_{dt} - \hat{y}_{dt}| < \beta \\ |y_{dt} - \hat{y}_{dt}| - \beta/2 & \text{otherwise} \end{cases}$$

and β is a hyperparameter.

Quantile Loss: Past studies found that Quantile loss can model non-Gaussian and asymmetric patterns in the data Wu et al. [2021], Mallick et al. [2022]. Let S be a set of fixed quantiles between 0 and 1. The Quantile Loss is defined as Koenker [2005], Wu et al. [2021]: $\sum_{\tau \in S} \sum_{d=1}^D \sum_{t=1}^T L_\tau(y_{dt}, \hat{y}_{dt})$ where $L_\tau(y_{dt}, \hat{y}_{dt}) = (y_{dt} - \hat{y}_{dt}) \cdot (\tau - \mathbf{1}(y_{dt} < \hat{y}_{dt}))$ for a fixed confidence level τ .

Balanced MSE: We adapt the Batch-based Monte-Carlo (BMC) implementation of the Balanced MSE Loss function Ren et al. [2022], which does not impose any assumptions on the label distribution. This loss function takes into account how rare the error is at the batch level. Given a batch of size B , we let \mathbf{y}_{bl} be a vector of length T , which represents the a sequence observed values of T times steps from the b th sample in the batch at the l th location. The BMC implementation of the Balanced MSE is defined as

$$-\log \frac{\exp(-\|\hat{\mathbf{y}}_{bl} - \mathbf{y}_{bl}\|_2^2 / (2\sigma_{\text{noise}}^2))}{\sum_{b'=1}^B \sum_{l'=1}^L \exp(-\|\hat{\mathbf{y}}_{bl} - \mathbf{y}_{b'l'}\|_2^2 / (2\sigma_{\text{noise}}^2))}$$

where σ_{noise}^2 is a hyperparameter. Even though Ren et al. [2022] suggest that σ_{noise}^2 can be learnt, it still requires another loss function to choose the best model tested on the validation set; however, this defeats the purpose of our study to find a good loss function both for training and validation.

Gumbel Loss: Proposed by Zhang et al. [2021], the Gumbel Loss is defined as $\frac{1}{T} \sum_{t=1}^T (1 - \exp(-\delta_{lt}^2))^\gamma \delta_{lt}^2$, where $\delta_{lt} = y_{dt} - \hat{y}_{dt}$ and γ is a hyperparameter. Notice that with $\gamma > 1$, it discounts smaller errors more aggressively than the MSE and is thus more sensitive to "outliers."

Kurtosis Loss: Kurtosis measures the tailedness of a distribution as the scaled fourth moment about the mean. Given a pre-defined loss function L , the Kurtosis in Kozerawski et al. [2022] is defined as $L + \lambda \cdot \left(\frac{\hat{L} - \mu_{\hat{L}}}{\sigma_{\hat{L}}}\right)^4$ where \hat{L} is the auxiliary loss and λ is a hyperparameter. $\mu_{\hat{L}}$ and $\sigma_{\hat{L}}$ are the mean and standard deviation of the loss \hat{L} for a batch of training samples. Kozerawski et al. [2022] suggest choosing the negative likelihood loss for \hat{L} ; however, it is unclear which distribution to choose for the negative likelihood loss. Even though, for example, the generalized Pareto distribution is chosen, it is unclear how to estimate the hyperparameters for traffic speed data.

Data	Model	Losses	15 min			30 min			60 min		
			MAE	RMSE	MAPE	MAE	RMSE	MAPE	MAE	RMSE	MAPE
METR-LA	GraphWaveNet	MAE	2.708	5.193	7.036	3.084	6.238	8.505	3.533	7.374	10.091
		MAE-Focal	2.749	5.120	7.111	3.127	6.127	8.438	3.595	7.216	9.982
		Quantile	2.693	5.139	6.966	3.074	6.137	8.393	3.552	7.278	10.032
		Huber	2.722	5.179	6.931	3.129	6.273	8.451	3.580	7.392	10.026
		MSE	2.870	5.117	7.438	3.307	6.078	8.815	3.846	7.069	10.324
		MSE-Focal	3.004	5.121	7.620	3.450	6.038	9.191	3.967	7.023	10.826
		bMSE-1	2.957	5.172	7.294	3.412	6.091	8.832	4.060	7.232	10.889
		bMSE-9	2.982	5.153	7.673	3.400	6.031	9.350	4.193	7.142	11.730
		Gumbel	2.881	5.070	7.498	3.324	6.017	9.069	3.846	7.028	10.870
	Kurtosis	2.910	5.940	7.468	3.446	7.313	9.317	4.260	9.058	12.095	
	D2STGNN	MAE	2.555	4.893	6.485	2.903	5.901	7.870	3.350	7.080	9.757
		MAE-Focal	2.595	4.869	6.582	2.945	5.864	7.943	3.395	6.956	9.639
		Quantile	2.557	4.882	6.513	2.908	5.904	7.902	3.355	7.003	9.642
		Huber	2.559	4.904	6.541	2.906	5.914	7.944	3.360	7.114	9.936
		MSE	2.685	4.844	6.815	3.067	5.769	8.211	3.633	6.787	10.101
		MSE-Focal	2.927	4.955	7.358	3.318	5.911	8.803	3.775	6.911	10.357
		bMSE-1	2.705	4.895	6.879	3.095	5.820	8.261	3.657	6.842	10.350
		bMSE-9	2.823	4.968	7.073	3.175	5.844	8.389	3.890	6.906	10.639
Gumbel		2.674	4.837	6.788	3.056	5.770	8.201	3.584	6.769	10.070	
Kurtosis	2.787	5.736	6.908	3.280	7.034	8.418	4.001	8.602	10.550		
PEMS-BAY	GraphWaveNet	MAE	1.310	2.748	2.741	1.641	3.701	3.674	1.964	4.497	4.594
		MAE-Focal	1.336	2.727	2.790	1.673	3.666	3.748	2.009	4.498	4.759
		Quantile	1.321	2.748	2.743	1.667	3.734	3.777	1.997	4.547	4.831
		Huber	1.324	2.756	2.757	1.675	3.767	3.707	2.019	4.605	4.676
		MSE	1.374	2.714	2.925	1.712	3.590	3.849	2.035	4.304	4.804
		MSE-Focal	1.450	2.759	3.069	1.804	3.643	3.957	2.120	4.314	4.836
		bMSE-1	1.417	2.747	2.947	1.744	3.622	3.837	2.122	4.422	4.872
		bMSE-9	1.473	2.783	3.064	1.780	3.647	3.960	2.501	4.738	5.519
		Gumbel	1.371	2.707	2.846	1.724	3.617	3.863	2.044	4.369	4.795
	Kurtosis	1.870	4.892	3.899	2.238	5.543	4.873	2.708	6.370	6.012	
	D2STGNN	MAE	1.253	2.631	2.621	1.566	3.578	3.539	1.881	4.354	4.361
		MAE-Focal	1.284	2.623	2.663	1.604	3.568	3.572	1.932	4.314	4.418
		Quantile	1.253	2.630	2.621	1.565	3.573	3.545	1.876	4.319	4.357
		Huber	1.258	2.631	2.631	1.572	3.571	3.567	1.879	4.316	4.391
		MSE	1.348	2.688	2.851	1.666	3.552	3.746	1.987	4.259	4.573
		MSE-Focal	1.429	2.729	2.955	1.794	3.626	3.916	2.138	4.355	4.833
		bMSE-1	1.383	2.742	2.961	1.722	3.618	3.867	2.093	4.425	4.801
		bMSE-9	1.532	2.838	3.207	1.836	3.663	4.087	2.501	4.685	5.522
Gumbel		1.322	2.677	2.782	1.659	3.622	3.721	1.997	4.344	4.628	
Kurtosis	1.392	3.103	2.970	2.092	5.162	4.476	2.893	6.820	6.114		

Table 1: This table compares the overall performance of loss functions with MAE, RMSE, MAPE. Against MAE, the MAE-Focal Loss often show similar MAE and MAPE performance but consistently lower RMSE. Meanwhile, the Gumbel Loss often outperforms MSE or exhibits similar results.

3.2 Evaluation Metrics

We evaluate all models for 15 minutes (3 steps), 30 minutes (6 steps) and 1 hour (12 steps) ahead forecasting. We first consider three traditional evaluation metrics for traffic forecasting: Mean Absolute Error (MAE), Root Mean Squared Error (RMSE), and Mean Absolute Percentage Error (MAPE) Li et al. [2018]. These metrics enable us to gauge the average predictive performance over the entire evaluation timeframe. In addition to these standard performance metrics, we introduce metrics designed to capture the model’s performance during abrupt speed fluctuations due to traffic congestion.

Identifying Bimodality in a Time Series. The first step to capture congestion is to focus on sensor locations that consistently display congestion patterns. To achieve this, we assess the bimodality in the empirical distribution of traffic speed time series data from each location. First, we utilize Kernel Density Estimation (KDE) to smooth the histogram

Data	Model	Losses	15 min			30 min			60 min		
			MAE	RMSE	MAPE	MAE	RMSE	MAPE	MAE	RMSE	MAPE
METR-LA	GraphWaveNet	MAE	6.741	10.882	17.240	8.092	13.042	20.784	9.138	14.615	24.251
		MAE-Focal	6.667	10.610	16.784	7.921	12.606	20.406	8.815	13.932	23.560
		Quantile	6.794	10.905	17.195	8.036	12.845	20.837	8.941	14.215	24.010
		Huber	6.730	10.754	17.620	8.058	12.880	21.095	9.032	14.346	24.477
		MSE	6.765	10.233	16.798	7.904	11.909	19.777	8.725	13.100	22.851
		MSE-Focal	6.985	10.486	17.323	8.120	12.157	20.019	8.765	13.030	22.019
		bMSE-1	7.049	10.557	18.848	8.105	12.053	21.205	8.811	13.061	22.753
		bMSE-9	7.026	10.437	17.668	8.053	11.898	19.238	8.671	12.702	19.312
		Gumbel	6.840	10.330	16.895	7.922	11.883	19.288	8.712	13.058	21.167
	Kurtosis	8.030	13.179	22.028	9.814	15.620	27.456	10.881	16.850	30.036	
	D2STGNN	MAE	6.094	10.068	15.597	7.387	12.216	18.880	8.519	13.965	21.300
		MAE-Focal	6.072	9.922	15.372	7.337	12.015	18.546	8.477	13.704	21.985
		Quantile	6.063	10.023	15.353	7.370	12.156	18.652	8.480	13.787	21.469
		Huber	6.095	10.098	15.480	7.347	12.167	18.511	8.603	14.103	21.160
		MSE	6.169	9.684	15.481	7.353	11.545	18.393	8.452	12.975	21.161
		MSE-Focal	6.360	9.711	15.657	7.522	11.558	18.509	8.408	12.935	21.255
		bMSE-1	6.209	9.684	15.685	7.381	11.536	18.591	8.316	12.806	20.106
		bMSE-9	6.326	9.739	17.182	7.409	11.504	18.672	8.378	12.684	20.133
Gumbel		6.146	9.626	15.289	7.322	11.482	18.140	8.308	12.809	20.524	
Kurtosis	7.446	12.436	20.828	9.079	14.681	26.375	10.041	15.826	29.294		
PEMS-BAY	GraphWaveNet	MAE	3.024	5.172	6.821	3.737	6.462	8.583	4.359	7.612	10.415
		MAE-Focal	3.001	5.071	6.692	3.721	6.359	8.361	4.404	7.696	9.928
		Quantile	2.982	5.072	6.875	3.756	6.445	8.729	4.312	7.462	9.783
		Huber	2.939	5.093	6.612	3.724	6.546	8.685	4.388	7.700	10.522
		MSE	2.994	4.913	6.652	3.728	6.139	8.343	4.228	7.080	9.414
		MSE-Focal	3.018	4.880	6.660	3.754	6.138	8.393	4.174	6.880	9.455
		bMSE-1	3.051	4.942	6.979	3.742	6.175	8.578	4.254	7.171	9.714
		bMSE-9	3.166	4.982	7.205	3.783	6.165	8.461	4.653	7.368	10.374
		Gumbel	2.963	4.869	6.683	3.675	6.065	8.268	4.167	7.069	9.435
	Kurtosis	4.262	7.966	10.870	5.299	9.417	13.089	6.267	10.677	15.287	
	D2STGNN	MAE	2.664	4.678	5.984	3.320	5.910	7.596	3.853	6.796	9.008
		MAE-Focal	2.679	4.607	6.057	3.370	5.889	7.763	3.874	6.734	9.104
		Quantile	2.684	4.728	6.034	3.364	6.005	7.681	3.900	6.896	9.143
		Huber	2.661	4.668	5.974	3.337	5.925	7.581	3.798	6.662	8.661
		MSE	2.928	4.820	6.513	3.592	5.980	8.043	3.980	6.686	9.059
		MSE-Focal	2.996	4.818	6.803	3.690	5.942	8.514	4.029	6.518	9.374
		bMSE-1	3.081	5.002	6.980	3.702	6.071	8.490	4.105	6.791	9.419
		bMSE-9	3.206	4.988	7.099	3.667	5.918	8.260	4.416	6.881	9.808
Gumbel		2.784	4.692	6.248	3.518	5.989	8.020	4.010	6.786	9.138	
Kurtosis	3.459	6.270	8.145	5.089	9.160	12.630	6.252	10.758	16.103		

Table 2: This table compares the performance of loss functions with MAE, RMSE, MAPE at identified congestion scenarios. Against MAE, the MAE-Focal Loss often show similar MAE and MAPE performance but consistently lower RMSE. Meanwhile, the Gumbel Loss often outperforms MSE or exhibits similar results.

of historical traffic speed. After smoothing, we locate all the local minima that are distanced at least 10 units (mph) from the mode of this curve. For each identified local minima, we compute the percentage of historical speeds below the speed represented by the minima. A time series is deemed to exhibit a *significant* bimodal distribution if a local minima exists and the calculated proportion exceeds 0.1.

Errors in Congested Scenarios: After all the sensor locations with significant bimodal distribution patterns are identified, we employ offline change point detection to identify the time steps marking the changes in traffic speed Aminikhanghahi and Cook [2017]. In particular, we employ the linearly penalized segmentation algorithm Killick et al. [2012] with the radial basis function (RBF) kernel Garreau and Arlot [2018], Arlot et al. [2019] provided by the ruptures Python package Truong et al. [2020]. Traffic speed changes can span across an interval, while change point detection methods may only identify a point within such an interval. To mitigate this issue, we introduce the “change point intervals,” where we incorporate two-time steps preceding and following each identified change point. Upon

Data	Model	Losses	15 min			30 min			60 min		
			95%	98%	99%	95%	98%	99%	95%	98%	99%
METR-LA	GraphWaveNet	MAE	9.769	17.009	23.599	11.843	22.101	30.149	14.971	28.111	36.373
		MAE-Focal	9.698	16.557	22.922	11.729	21.407	29.157	14.658	26.873	35.021
		Quantile	<u>9.722</u>	16.789	23.221	<u>11.759</u>	21.467	29.154	<u>14.771</u>	27.169	35.437
		Huber	9.843	16.968	23.462	12.091	22.297	30.115	15.072	27.931	36.201
		MSE	10.288	16.486	21.799	12.517	20.632	26.981	15.136	24.811	31.787
		MSE-Focal	10.153	16.260	21.584	12.205	20.069	26.574	14.910	<u>24.300</u>	<u>30.965</u>
		bMSE-1	10.422	16.689	22.034	12.769	20.407	26.396	15.772	<u>24.886</u>	31.438
		bMSE-9	10.354	16.436	<u>21.571</u>	12.606	<u>20.093</u>	26.003	15.363	24.007	30.399
		Gumbel	10.167	<u>16.275</u>	21.555	12.436	20.248	26.459	15.099	24.485	31.279
	Kurtosis	10.434	21.169	30.852	13.941	30.573	37.648	23.009	37.430	40.220	
	D2STGNN	MAE	9.103	15.586	22.027	<u>10.773</u>	20.420	28.683	<u>13.636</u>	26.805	35.645
		MAE-Focal	9.026	15.401	21.808	10.729	20.244	28.402	13.452	25.951	34.728
		Quantile	<u>9.083</u>	15.566	21.934	10.819	20.415	28.736	13.676	26.167	34.729
		Huber	9.108	15.639	22.110	10.805	20.499	28.801	13.714	26.821	35.759
		MSE	9.305	15.270	20.896	11.151	19.357	<u>26.477</u>	13.993	23.871	31.327
		MSE-Focal	9.547	15.430	20.823	11.522	19.684	<u>26.613</u>	14.268	24.310	31.651
		bMSE-1	9.512	15.538	20.996	11.346	19.555	26.580	14.246	24.022	31.259
		bMSE-9	9.654	15.601	21.026	11.392	19.434	26.388	14.249	23.727	30.935
Gumbel		9.333	<u>15.271</u>	<u>20.862</u>	11.178	<u>19.406</u>	26.497	13.950	<u>23.867</u>	<u>31.241</u>	
Kurtosis	9.771	19.936	30.388	12.745	29.618	37.587	20.094	37.102	39.623		
PEMS-BAY	GraphWaveNet	MAE	4.497	8.557	12.567	5.956	12.124	17.971	<u>7.403</u>	15.426	22.478
		MAE-Focal	4.545	8.417	12.285	<u>5.964</u>	11.778	17.498	7.402	15.139	22.307
		Quantile	4.537	8.560	12.522	<u>6.070</u>	12.293	18.134	7.500	15.533	22.584
		Huber	<u>4.519</u>	8.566	12.540	5.996	12.316	18.435	7.512	15.826	23.283
		MSE	4.863	8.640	12.054	6.395	11.855	<u>16.669</u>	7.806	<u>14.573</u>	<u>20.313</u>
		MSE-Focal	5.036	8.694	<u>12.060</u>	6.510	<u>11.811</u>	16.587	7.839	14.310	20.060
		bMSE-1	4.903	8.660	12.165	6.474	11.897	16.722	8.018	14.835	20.722
		bMSE-9	4.910	8.773	12.247	6.429	12.014	17.000	8.065	15.040	21.077
		Gumbel	4.743	<u>8.490</u>	12.066	6.339	11.833	16.832	7.749	14.720	20.785
	Kurtosis	6.490	23.633	29.274	9.540	26.426	29.659	14.532	28.102	30.184	
	D2STGNN	MAE	4.233	8.000	11.900	5.536	11.244	17.149	<u>6.864</u>	14.421	21.641
		MAE-Focal	4.306	7.908	11.643	5.589	11.112	16.849	<u>6.910</u>	14.097	21.088
		Quantile	4.244	8.003	<u>11.867</u>	5.569	11.284	17.078	6.956	14.351	21.227
		Huber	4.239	7.969	11.892	<u>5.553</u>	<u>11.237</u>	17.037	6.841	14.270	21.304
		MSE	4.710	8.464	11.986	6.135	11.493	<u>16.417</u>	7.482	14.204	<u>20.142</u>
		MSE-Focal	4.908	8.495	11.931	6.492	11.647	16.403	7.814	<u>14.183</u>	20.015
		bMSE-1	4.830	8.681	12.281	6.408	11.736	16.607	7.930	<u>14.625</u>	20.452
		bMSE-9	5.126	8.910	12.389	6.585	11.880	16.602	8.541	14.898	20.681
Gumbel		4.546	8.266	11.890	5.994	11.536	16.893	7.482	14.497	20.754	
Kurtosis	4.600	9.483	15.325	8.180	23.664	29.210	17.629	29.241	30.688		

Table 3: This table compares the VaR of each loss function at three different levels: 95%, 98%, and 99%. first-order losses yield smaller errors at the 95th percentile. However, at the 99th percentile, second-order losses are often superior, suggesting they are more effective for managing extreme errors.

the identification of change point intervals, we calculate the MAE, RMSE, and MAPE to assess performance at these intervals.

Value-at-Risk Metric: We adapt the Value-at-Risk (VaR) Resnick [2007], Kozerawski et al. [2022] metric commonly used in heavy-tail analysis: given $\alpha \in (0, 1)$, the VaR at the level α is defined as: $\text{VaR}_\alpha(E) = \inf\{e \in E : \mathbb{P}(E \geq e) \leq 1 - \alpha\}$ i.e. the smallest error e such that the probability of observing error larger than e is smaller than $1 - \alpha$, where E is the empirical distribution of error in the test set. This reports the α -th quantile of the error distribution. We use the absolute error: $|y_{cdt} - \hat{y}_{cdt}|$ for e and measure VaR at three different levels: 95%, 98%, and 99%.

4 Experiments

Datasets: Our research is based on two traffic speed datasets, METR-LA Jagadish et al. [2014] and PEMS-BAY Chen et al. [2001], first benchmarked by Li et al. [2018]. METR-LA contains observations from $D = 207$ sensors

Horizon	Loss	MAE					MSE				
		Overall		Congestion			Overall		Congestion		
		MAE	RMSE	MAE	RMSE	Extreme VaR Errors	MAE	RMSE	MAE	RMSE	Extreme VaR Errors
15 min	MAE-Focal	✓	✓✓	✓✓	✓✓	✓✓	✓✓	✓	✓✓		
	Quantile	✓	✓✓	✓	✓	✓✓	✓✓	✓	✓✓		
	Huber	✓	✓	✓✓	✓✓	✓✓	✓✓	✓	✓✓		
	MSE-Focal		✓✓			✓✓				✓	✓✓
	bMSE						✓	✓			
	Gumbel		✓✓		✓✓	✓✓	✓✓	✓✓	✓✓	✓✓	✓✓
	Kurtosis										
30 min	MAE-Focal	✓	✓✓	✓✓	✓✓	✓✓	✓✓	✓	✓		
	Quantile	✓	✓	✓	✓		✓✓				
	Huber	✓	✓	✓	✓✓		✓✓				
	MSE-Focal		✓		✓	✓✓					✓✓
	bMSE		✓✓		✓	✓✓	✓	✓		✓✓	✓
	Gumbel		✓✓		✓✓	✓✓	✓	✓	✓✓	✓✓	✓
	Kurtosis										
1 hour	MAE-Focal	✓	✓✓	✓	✓✓		✓✓				
	Quantile	✓	✓✓	✓✓	✓✓		✓✓				
	Huber	✓	✓	✓			✓✓				
	MSE-Focal		✓✓		✓✓				✓	✓✓	✓✓
	bMSE		✓✓		✓✓				✓	✓	✓
	Gumbel		✓✓		✓✓		✓	✓	✓✓	✓✓	✓
	Kurtosis										

Table 4: Comparison of different loss functions benchmarked against MAE and MSE Losses. A single check mark denotes error rates comparable to or better than MAE or MSE, with a difference of up to 0.1. Double check marks signify consistently lower errors, except for at most 1 entry. The 99th quantile of VaR errors is considered extreme. **Against MAE, the MAE-Focal Loss shows similar MAE performance but consistently lower RMSE. Against MSE, the Gumbel Loss has similar MAE and RMSE results but lower errors during congestion periods.**

over 4 months and 82 of the 207 (39.6%) sensors exhibit a significant bimodal distribution in their historical speeds. PEMS-BAY contains observations from $D = 325$ sensors in the Bay Area over 6 months and 79 of the 325 (24.3%) sensors exhibit a significant bimodal distribution in their historical speeds. Overall, the traffic presented in PEMS-BAY is less congested than that in METR-LA.

Experiment Setup: We choose two state-of-the-art models for traffic speed forecasting for this study: GraphWaveNet Wu et al. [2019] and D2STGNN Shao et al. [2022]. We adhere to the same setup as described in their original papers. We remark that GraphWaveNet is executable with Pytorch version between 1.3.1 and 1.9.0 and is trained for 100 epochs. D2STGNN is executable with Pytorch version 1.9.1 or later and is trained for 80 epochs. All experiments are carried out on an NVIDIA DGX A100.

Implementation Details: Based on the original implementation, we select the following specifications for loss functions: Focal Loss $\beta = 0.2$ and $\gamma = 1$; Quantile Loss Wu et al. [2021] $S = \{0.025, 0.5, 0.975\}$; Huber Loss $\beta = 1$; Balanced MSE: σ_{noise}^2 to be 1 and 9 (we refer the Balanced MSE Loss with $\sigma_{\text{noise}}^2 = 1$ as bMSE-1 and the other as bMSE-9); Gumbel Loss: $\gamma = 1.1$; Kurtosis Loss: l is the MAE loss, \hat{l} is the MSE Loss and $\lambda = 0.01$.

4.1 Results

Table 1 presents a comparison of the overall performance of various loss functions. We divide the first-order losses from second-order losses and align Kurtosis Loss with the second-order loss for a more straightforward visualization. The best-performing loss function within each group is highlighted in bold. We observe that first-order losses generally perform better in MAE, while second-order losses excel in RMSE. Moreover, the MAE-Focal Loss often outperforms the standard MAE Loss in terms of RMSE. The difference in MAE values between the two can be as significant as 0.1. Meanwhile, Gumbel Loss often displays superior performance to Mean Square Error (MSE) in terms of RMSE, and sometimes in terms of MAE.

Table 2 is similar to Table 1, except that the prior evaluates the performance of these loss functions specifically in identified traffic congestion scenarios. We observe a notably higher performance of MAE-Focal Loss compared to

standard MAE Loss. This can be explained by MAE-Focal Loss placing more emphasis on penalizing rare labels, representative of traffic speeds during congested periods. Meanwhile, the Gumbel Loss tends to exhibit a lower RMSE compared to MSE more frequently. This is due to its factor, $(1 - \exp(-\delta_{it}^2))^\gamma$, which significantly discounts smaller errors, pushing the model to focus on larger errors. Moreover, for both loss functions, improvements on the PEMS-BAY dataset are less pronounced, possibly because traffic in the Bay area is generally less congested.

Interestingly, in congested scenarios (Table 2), second-order losses can occasionally outperform in MAE for longer durations (30 min and 1 hour). This can be attributed to that as predictions extend further into the future, second-order losses impose greater penalties on large errors, leading to more aggressive corrections.

Table 3 compares the Value-at-Risk (VaR) of each loss function across three levels: 95%, 98%, and 99%. We do not group the loss functions for easier visualization. The bold font indicates the best performer and the underline indicates the second best. First-order losses generally yield smaller errors at the 95th percentile, indicating better performance for typical speed observations. Also, the MAE-Focal Loss often outperforms the standard MAE Loss at the 98th and 99th percentiles. On the other hand, second-order losses tend to have smaller errors at the 99th percentile, hinting at their potential in mitigating larger errors. Among them, MSE-Focal tend to produce lower errors across various time horizons. However, no second-order loss consistently outperforms others, making the search for a loss function resilient to large errors in traffic speed data an interesting research question.

As a summary, we benchmark all loss functions against MAE and MSE in Table 4: **against MAE, MAE-Focal Loss is recommended due to its comparable MAE but consistently lower RMSE in both general and congested scenarios; against MSE, the Gumbel Loss is recommended, given its similar MAE and RMSE in general scenarios but superior performance during congested periods.**

5 Conclusion

In this study, we perform benchmark analyses to assess the efficacy of multiple loss functions in traffic forecasting, emphasizing their ability to forecast congestion, a significant challenge faced by existing AI systems. These evaluations are carried out on two datasets, META-LA and PEMS-BAY, leading us to the following recommendation: for objectives centered on the optimization of MAE, we recommend the MAE-Focal Loss function; for objectives directed toward the optimization of MSE, we recommend the Gumbel Loss. These loss functions enhance deep learning models' efficacy in predicting traffic congestion by incorporating techniques from imbalanced regression and extreme value theory.

For future work, a crucial area for improvement lies in optimizing the hyperparameter selection, as a more refined hyperparameter tuning approach can help fully harness the capabilities of these novel loss functions. Moreover, heavy tail analysis in the context of traffic speed forecasting is under explored. Thus, one interesting research question is adapting the Generalised Pareto distribution to account for the complex spatiotemporal dependencies in the traffic speed data.

It's imperative to underline that by enhancing the prediction accuracy for congestion, we're paving the way for AI systems that are not only more accurate but also safe, robust, and responsible in real-world applications.

Acknowledgments

This material is based on research supported by a project under the Sustainable Research Pathways (SRP) Program. This research used resources from the Argonne Leadership Computing Facility, which is a DOE Office of Science User Facility under contract DE-AC02-06CH11357. The authors would like to extend their gratitude to Prasanna Balaprakash and Ngoc Mai Tran for their valuable suggestions regarding the methodology of this study.

Government license

The submitted manuscript has been created by UChicago Argonne, LLC, Operator of Argonne National Laboratory ("Argonne"). Argonne, a U.S. Department of Energy Office of Science laboratory, is operated under Contract No. DE-AC02-06CH11357. The U.S. Government retains for itself, and others acting on its behalf, a paid-up nonexclusive, irrevocable worldwide license in said article to reproduce, prepare derivative works, distribute copies to the public, and perform publicly and display publicly, by or on behalf of the Government. The Department of Energy will provide public access to these results of federally sponsored research in accordance with the DOE Public Access Plan. <http://energy.gov/downloads/doe-public-access-plan>.

References

- Yaguang Li, Rose Yu, Cyrus Shahabi, and Yan Liu. Diffusion convolutional recurrent neural network: Data-driven traffic forecasting. In *ICLR*, 2018.
- Zonghan Wu, Shirui Pan, Guodong Long, Jing Jiang, and Chengqi Zhang. Graph wavenet for deep spatial-temporal graph modeling. In *Proceedings of the 28th International Joint Conference on Artificial Intelligence*, pages 1907–1913, 2019.
- ZeZhi Shao, Zhao Zhang, Wei Wei, Fei Wang, Yongjun Xu, Xin Cao, and Christian S Jensen. Decoupled dynamic spatial-temporal graph neural network for traffic forecasting. *Proceedings of the VLDB Endowment*, 15(11):2733–2746, 2022.
- Mourad Lablack and Yanming Shen. Spatio-temporal graph mixformer for traffic forecasting. *Expert Systems with Applications*, 228:120281, 2023.
- Daizong Ding, Mi Zhang, Xudong Pan, Min Yang, and Xiangnan He. Modeling extreme events in time series prediction. In *Proceedings of the 25th ACM SIGKDD International Conference on Knowledge Discovery & Data Mining*, pages 1114–1122, 2019.
- Rita P Ribeiro and Nuno Moniz. Imbalanced regression and extreme value prediction. *Machine Learning*, 109(9):1803–1835, 2020.
- Richard Bishop. *Intelligent vehicle technology and trends*. 2005.
- Shuming Tang and Haijun Gao. Traffic-incident detection-algorithm based on nonparametric regression. *IEEE Transactions on Intelligent Transportation Systems*, 6(1):38–42, 2005.
- Fitsum Teklu, Agachai Sumalee, and David Watling. A genetic algorithm approach for optimizing traffic control signals considering routing. *Computer-Aided Civil and Infrastructure Engineering*, 22(1):31–43, 2007.
- Mi Zhang, Daizong Ding, Xudong Pan, and Min Yang. Enhancing time series predictors with generalized extreme value loss. *IEEE Transactions on Knowledge and Data Engineering*, 2021.
- Jedrzej Kozerawski, Mayank Sharan, and Rose Yu. Taming the long tail of deep probabilistic forecasting. *arXiv preprint arXiv:2202.13418*, 2022.
- Yuzhe Yang, Kaiwen Zha, Ying-Cong Chen, Hao Wang, and Dina Katabi. Delving into deep imbalanced regression. *ICML*, 2021.
- Jiawei Ren, Mingyuan Zhang, Cunjun Yu, and Ziwei Liu. Balanced mse for imbalanced visual regression. In *Proceedings of the IEEE/CVF Conference on Computer Vision and Pattern Recognition*, pages 7926–7935, 2022.
- Kyunghyun Cho, Bart van Merriënboer, Dzmitry Bahdanau, and Yoshua Bengio. On the properties of neural machine translation: Encoder-decoder approaches. In *SSST@EMNLP*, pages 103–111, 2014.
- Fisher Yu and Vladlen Koltun. Multi-scale context aggregation by dilated convolutions. In *4th International Conference on Learning Representations, ICLR 2016, San Juan, Puerto Rico, May 2-4, 2016, Conference Track Proceedings*, 2016.
- Jiani Zhang, Xingjian Shi, Junyuan Xie, Hao Ma, Irwin King, and Dit-Yan Yeung. Gaan: Gated attention networks for learning on large and spatiotemporal graphs. In *Proceedings of the Thirty-Fourth Conference on Uncertainty in Artificial Intelligence, UAI 2018, Monterey, California, USA, August 6-10, 2018*, pages 339–349, 2018.
- Bing Yu, Haoteng Yin, and Zhanxing Zhu. Spatio-temporal graph convolutional networks: a deep learning framework for traffic forecasting. In *Proceedings of the 27th International Joint Conference on Artificial Intelligence*, pages 3634–3640, 2018.
- Tanwi Mallick, Mariam Kiran, Bashir Mohammed, and Prasanna Balaprakash. Dynamic graph neural network for traffic forecasting in wide area networks. In *2020 IEEE International Conference on Big Data (Big Data)*, pages 1–10. IEEE, 2020a.
- Tanwi Mallick, Prasanna Balaprakash, Eric Rask, and Jane Macfarlane. Graph-partitioning-based diffusion convolutional recurrent neural network for large-scale traffic forecasting. *Transportation Research Record*, 2674(9):473–488, 2020b.
- Ge Zheng, Wei Koong Chai, Jing-Lin Duanmu, and Vasilis Katos. Hybrid deep learning models for traffic prediction in large-scale road networks. *Information Fusion*, 92:93–114, 2023.
- Tanwi Mallick, Prasanna Balaprakash, Eric Rask, and Jane Macfarlane. Transfer learning with graph neural networks for short-term highway traffic forecasting. In *2020 25th International Conference on Pattern Recognition (ICPR)*, pages 10367–10374. IEEE, 2021.

- Yunjie Huang, Xiaozhuang Song, Shiyao Zhang, and JQ James. Transfer learning in traffic prediction with graph neural networks. In *2021 IEEE International Intelligent Transportation Systems Conference (ITSC)*, pages 3732–3737. IEEE, 2021.
- Tanwi Mallick, Prasanna Balaprakash, and Jane Macfarlane. Deep-ensemble-based uncertainty quantification in spatiotemporal graph neural networks for traffic forecasting. *arXiv preprint arXiv:2204.01618*, 2022.
- Laurens Haan and Ana Ferreira. *Extreme value theory: an introduction*, volume 3. Springer, 2006.
- Meryem Tanarhte, Panos Hadjinicolaou, and Jos Lelieveld. Heat wave characteristics in the eastern mediterranean and middle east using extreme value theory. *Climate Research*, 63(2):99–113, 2015.
- Roger Koenker. *Quantile regression*, volume 38. Cambridge university press, 2005.
- Stephen Wambura, He Li, and Alemu Nigussie. Fast memory-efficient extreme events prediction in complex time series. In *Proceedings of the 2020 3rd International Conference on Robot Systems and Applications*, pages 60–69, 2020.
- Michael Steininger, Konstantin Kobs, Pdraig Davidson, Anna Krause, and Andreas Hotho. Density-based weighting for imbalanced regression. *Machine Learning*, 110(8):2187–2211, 2021.
- Xiankai Lu, Chao Ma, Bingbing Ni, Xiaokang Yang, Ian Reid, and Ming-Hsuan Yang. Deep regression tracking with shrinkage loss. In *Proceedings of the European conference on computer vision (ECCV)*, pages 353–369, 2018.
- Tsung-Yi Lin, Priya Goyal, Ross Girshick, Kaiming He, and Piotr Dollár. Focal loss for dense object detection. In *Proceedings of the IEEE international conference on computer vision*, pages 2980–2988, 2017.
- Peter J Huber. Robust estimation of a location parameter. In *Breakthroughs in statistics: Methodology and distribution*, pages 492–518. Springer, 1992.
- Dongxia Wu, Liyao Gao, Matteo Chinazzi, Xinyue Xiong, Alessandro Vespignani, Yi-An Ma, and Rose Yu. Quantifying uncertainty in deep spatiotemporal forecasting. In *Proceedings of the 27th ACM SIGKDD Conference on Knowledge Discovery & Data Mining*, pages 1841–1851, 2021.
- Samaneh Aminikhanghahi and Diane J Cook. A survey of methods for time series change point detection. *Knowledge and information systems*, 51(2):339–367, 2017.
- Rebecca Killick, Paul Fearnhead, and Idris A Eckley. Optimal detection of changepoints with a linear computational cost. *Journal of the American Statistical Association*, 107(500):1590–1598, 2012.
- Damien Garreau and Sylvain Arlot. Consistent change-point detection with kernels. *Electronic Journal of Statistics*, 12(2):4440–4486, 2018.
- Sylvain Arlot, Alain Celisse, and Zaid Harchaoui. A kernel multiple change-point algorithm via model selection. *Journal of machine learning research*, 20(162), 2019.
- Charles Truong, Laurent Oudre, and Nicolas Vayatis. Selective review of offline change point detection methods. *Signal Processing*, 167:107299, 2020.
- Sidney I Resnick. *Heavy-tail phenomena: probabilistic and statistical modeling*. Springer Science & Business Media, 2007.
- Hosagrahar V Jagadish, Johannes Gehrke, Alexandros Labrinidis, Yannis Papakonstantinou, Jignesh M Patel, Raghu Ramakrishnan, and Cyrus Shahabi. Big data and its technical challenges. *Communications of the ACM*, 57(7):86–94, 2014.
- Chao Chen, Karl Petty, Alexander Skabardonis, Pravin Varaiya, and Zhanfeng Jia. Freeway performance measurement system: mining loop detector data. *Transportation Research Record*, 1748(1):96–102, 2001.